Available online at www.sciencedirect.com
ScienceDirect
Polymer 47 (2006) 7160–7165
polymer
www.elsevier.com/locate/polymer

Structure and vibrational frequency determination for α-poly(vinylidene fluoride) using density-functional theory

Nicholas J. Ramer*, Theresa Marrone, Kimberly A. Stiso[1]

Department of Chemistry, Long Island University, C.W. Post Campus, 720 Northern Boulevard, Brookville, NY 11548-1300, USA

Received 2 July 2006; received in revised form 31 July 2006; accepted 7 August 2006
Available online 24 August 2006

Abstract

The structure of the non-polar α-phase of poly(vinylidene fluoride) (PVDF) is determined by density-functional methods. We find very good agreement between our relaxed structure and that of previous X-ray diffraction studies. Using the relaxed structure, we have determined the infrared and Raman frequencies for the material using density-functional perturbation theory. The resulting frequencies are in excellent agreement with experiment and are comparable in accuracy to semi-empirical values for most absorbencies. In addition, we find a better agreement to experiment than a previously reported Hartree–Fock determination of vibrational frequencies in finite isolated PVDF chains. The low-frequency portion of our spectra (50–300 cm^{-1}) shows better agreement with experimental values than the same frequencies found semi-empirically. Improved accuracy in this frequency range will aid in modeling phase transitions and dielectric response in PVDF.

Keywords: Fluorinated polymers; Density-functional theory; Vibrational frequencies

1. Introduction

Poly(vinylidene fluoride) or PVDF exhibits polymorphism with at least five phases found experimentally [1]. The β-phase (form I) has been the most highly studied due to its ferroelectric, piezoelectric and pyroelectric behaviors. The α-phase (form II), which is non-polar, does not exhibit ferroelectricity. However, high-pressure heat treatment of the α-phase causes reorientation of its polymer chains to yield the γ-phase (form II_p or IV), which is ferroelectric [2]. Similarly, it has been shown that a phase transition from α to β can be produced when samples are subjected to high electric fields (nearly 5 MV/cm) [3], or placed under compressive or tensile stress [4–6].

The different phases of PVDF can be characterized by the conformations of the $-CH_2-$ and $-CF_2-$ in the polymer chain. For example, the β-phase has only *trans* (*t*) conformations present in its polymer chains; so called all-*trans* (see Fig. 1(a)). Its chains are oriented with the $-CF_2-$ dipoles pointing along the *y*-axis. This alignment is the reason for the spontaneous polarization found in the β-phase. In other PVDF phases, such as α and γ, *gauche* conformations are also present with either direction of rotation possible (g^+ or g^-) (see Fig. 1(b) for α-PVDF structure) [1].

There are conflicting assignments for the space group of α-PVDF throughout the literature. An overview of the experimental findings for the α-PVDF space group assignment can be found in Ref. [7]. Using X-ray data, Doll and Lando [8] first proposed two possible structures with space groups $P2_1(C_2^2)$ and $P1(C_1^1)$ containing two chains with tg^+tg^- conformation pattern. The first of these proposed structures was termed parallel with both chains pointing in the same direction. The latter of the two proposed structures was termed antiparallel due to the presence of chains that are oriented in opposing directions. Hasegawa et al. [9] revisited the space group assignment and determined a slightly different antiparallel monoclinic structure with space group $P2_1/c(C_{2h}^5)$.

* Corresponding author. Tel.: +1 516 299 3034; fax: +1 516 299 3944.
E-mail address: nramer@liu.edu (N.J. Ramer).
[1] Present address: Department of Chemistry, St. John's University, 8000 Utopia Parkway, Queens, NY 11439, USA.

0032-3861/$ - see front matter © 2006 Elsevier Ltd. All rights reserved.
doi:10.1016/j.polymer.2006.08.012

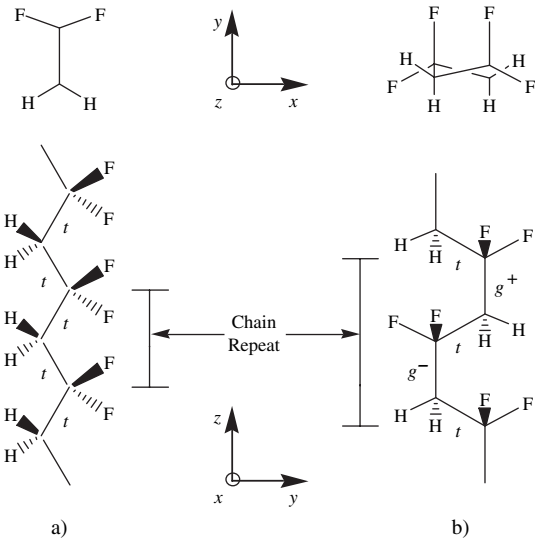

Fig. 1. Molecular structure (chain and side views) of poly(vinylidene fluoride) (a) β-phase, (b) α-phase (*t* is *trans* conformation and $g^{\pm}$ is *gauche* conformation with +/− rotation).

Subsequently, Bachmann and Lando reported that α-PVDF was a statistical orthorhombic structure with space group $P2cm(C_{2v}^4)$ in which up and down molecules occupy the same crystal site with equal probability [10]. This statistical structure, however, does not explain the X-ray diffraction pattern of tilt samples in which unequal intensities are observed for reflections that should possess equal intensities for an orthorhombic structure [11]. A possible explanation for these different space group determinations may lie in differing amounts of head-to-head followed by tail-to-tail units in the samples used by the two studies [12].

As a means to definitively assign the space group, Takahashi et al. [13] examined a uniaxially oriented sample that had been stretched and then annealed, as well as a tilt sample. Based upon these new intensity data, they proposed a different statistical monoclinic model ($P2_1/c$). The resulting model contains four molecules with different orientations; AC, A$\overline{\text{C}}$, $\overline{\text{A}}$C and $\overline{\text{AC}}$ where A and $\overline{\text{A}}$ indicate chain mirror images along the *a*-axis and C and $\overline{\text{C}}$ indicate chain mirror images along the *c*-axis. In this model, the four molecules have different existence percentages with molecule AC having the greatest probability (54%). Lastly, a more complex model was proposed in which regions of the samples are monoclinic $P2_1/c$ and orthorhombic $Pbc2_1(C_{2v}^5)$ [14]. This latter assignment implies that the crystals in this region are only periodic in the *b* and *c* directions.

The first experimental comparison study of the infrared spectra of the α- and β-phases was completed by Makarevich and Nikitin [15]. Subsequently, normal modes for both phases were determined using Urey–Bradley type force fields for the potential function which was fit to experimental results [16]. The observation of a temperature-dependent vibrational spectrum of PVDF was made by Wentink et al. [17]. Clarification of the origin of the temperature dependency was made by Cortili and Zerbi who identified the conformational differences between the α- and β-phases and identified unique modes in their respective infrared spectra [18]. Raman studies confirmed the chain conformations in α-PVDF proposed by Cortili and Zerbi and settled mode assignment ambiguities [19]. Based on this work, Boerio and Koenig [20] developed a valence force field model from transferred force constants of polyethylene [21] and polytetrafluoroethylene [22]. This model was used to determine the vibrational frequencies for the α- and β-phases. Tadokoro et al. modified the valence force field of Boerio and Koenig to include intermolecular interactions and determined frequencies in good agreement with experiment (see below) [23]. A recent re-determination using similar methods and a further modified force field of Boerio and Koenig yielded slightly different results [24].

Recently, a semi-empirical/quantum-mechanical approach was used to determine the infrared vibrational spectrum for α-PVDF [25]. In this study, the geometry of an isolated finite α-PVDF chain (20 monomers in length) was first studied using a semi-empirical application of Hartree–Fock theory called CNDO (Complete Neglect of Differential Overlap). Upon molecular optimization, a vibrational analysis was completed using CNDO and a simple harmonic oscillator model was used to determine the spectrum (see below). To our knowledge, a complete first-principles determination of the structure and vibrational spectrum of α-PVDF has not been reported.

PVDF has long been viewed as an important material not only for ferroelectric device applications but also more recently, in the development of fluoroelastomers. It is because of these reasons that a more detailed understanding of its structure and more importantly, its vibrational properties must be completed. Previous determinations of the vibrational frequencies of α-PVDF have relied on force constant or semi-empirical/quantum-mechanical models that were parameterized to experimental results. In the present study we have applied first-principles density-functional theory to determine the molecular structure of α-PVDF. We have used periodic boundary conditions to include intermolecular interactions. Density-functional perturbation theory is then employed to study the vibrational properties of the structure that resulted from the unconstrained relaxation. This yields both infrared and Raman frequencies. We will compare our frequencies to that of experiment and those found using semi-empirical and semi-empirical/quantum-mechanical methods.

2. Theoretical methodology

Density-functional theory (DFT) calculations were completed via the ABINIT software package [26,27]. The Perdew–Burke–Ernzerhof generalized-gradient approximation (GGA) [28] and periodic boundary conditions were also employed. Optimized pseudopotentials [29] were generated using the OPIUM code [30] for use with a plane-wave basis set cut-off energy of 50 Ry. Brillouin zone integrations were done using a $4 \times 4 \times 4$ Monkhorst–Pack *k*-point mesh [31]. A Broyden–Fletcher–Goldfarb–Shanno minimization algorithm was utilized for atomic relaxations [32]. Reported atomic positions possess less than 0.003 eV/Å residual Hellmann–Feynman

forces along each lattice direction [33]. Lattice parameter relaxation was done simultaneously with atomic relaxation by computing stress on the unit cell. Relaxation of the unit cell parameters (lattice constants and angles) was considered completed when total stress on the unit cell was less than 3 MPa. For the determination of the vibrational frequencies, density-functional perturbation theory was applied [34–38]. These same methods and pseudopotentials have been used previously to study the structure and vibrational frequencies of β-PVDF [39,40].

The unit cell for α-PVDF is monoclinic with $P2_1/c(C_{2h}^5)$ space group symmetry. We have chosen this symmetry due to its ability to describe the tilting phenomena found experimentally (see above). Each unit cell contains two antiparallel polymer chains, consisting of two monomers each. One chain is centered at the origin and the other at (0,1/2,1/2). Initial atomic positions and lattice parameters were taken from Ref. [9]. In the present study, due to space group symmetry, lattice angle β was allowed to deviate from 90°.

3. Results and discussions

3.1. Energetics and relaxed structure for α-PVDF

Upon full atomic and structural relaxation, the total energy of the α-phase of PVDF was approximately 0.027 eV per formula unit lower than the planar–zigzag β-phase. This same energy ordering was also found in a previous density-functional determination of PVDF phase energetics by Su et al. [41]. Quantitative comparison of the energy differences between the two phases is not possible since no information was provided regarding their relaxed structures.

Table 1 lists atomic positions for the relaxed structure of α-PVDF found in the present study. For comparison we have included the atomic positions from the X-ray diffraction study of Hasegawa et al. [2]. In these structures, C1 is bonded to the fluorine atoms and C2 is bonded to the hydrogen atoms. Table 2 lists lattice parameters as well as bond lengths and angles found in the present study and from experiment [2].

We find very good agreement between our relaxed structure and experiment. This agreement exists despite an increase in unit cell volume and the slight sheer found in unit cell ($\beta \neq 90°$). The over-estimation of the volume is commonly seen in GGA calculations. Even with our larger volume, we find most bond lengths and angles very close to their experimental values. Two notable exceptions are the C–F bond length and the H–C–H bond angle. It is important to note that due to thermal vibration, some uncertainty exists in the reported experimental positions. Since our DFT determination is considered to be for the 0 K structure, small deviations from experiment are expected. In addition, due to their small atomic size, the position of the hydrogen atoms may have greater ambiguity.

Table 1
Theoretical and experimental atomic positions for α-poly(vinylidene fluoride)

Atom	Present theory[a]			Experiment[b]		
	x/a	*y/b*	*z/c*	*x/a*	*y/b*	*z/c*
C1	0.322	0.193	0.168	0.308	0.186	0.150
C2	0.235	0.194	−0.146	0.238	0.183	−0.175
F1	0.589	0.178	0.187	0.576	0.178	0.185
F2	0.224	0.076	0.278	0.218	0.070	0.276
H1	0.023	0.191	−0.154	0.021	0.166	−0.194
H2	0.306	0.103	−0.239	0.366	0.096	−0.240

Positions are given as fractions of lattice constants. See text for atom identification.
[a] $a = 5.18$ Å; $b = 10.30$ Å; $c = 4.70$ Å; $\beta = 91°$.
[b] From Ref. [9] with $a = 4.96$ Å; $b = 9.64$ Å; $c = 4.62$ Å; $\beta = 90°$.

Table 2
Theoretical and experimental lattice constants and angles, bond lengths and angles for α-poly(vinylidene fluoride)

	Present theory	Experiment[a]
Lattice constants		
a	5.18	4.96
b	10.30	9.64
c	4.70	4.62
Lattice angle		
β	91	90
Bond lengths		
C–H	1.10	1.09
C–F	1.39	1.34
C–C	1.53	1.54
Bond angles		
H–C–H	107.2	114.6
F–C–F	105.3	103.2
C1–C2–C1	117.4	116.5
C2–C1–C2	118.5	118.5

Lattice constants and bond lengths are given in Angstroms, and lattice and bond angles in degrees. See text for atom identification.
[a] From Ref. [9].

3.2. Vibrational frequencies for α-PVDF

Based on group theory analysis, α-PVDF possesses 72 modes, 18 normal modes with A_g symmetry, 18 with B_g symmetry, 18 with A_u symmetry and 18 with B_u symmetry. For each symmetry species, the 18 modes can be divided into 16 molecular modes and 2 translational lattice modes. These translational lattice modes are either pure translational or librational. The pure translational mode along the *b*-axis belongs to symmetry species A_u and the pure translational modes along the *a*- and *c*-axes belong to species B_u. The A_g and B_g modes are infrared silent but Raman active. The A_u and B_u modes are infrared active but Raman silent.

Table 3 lists the infrared and Raman frequencies for α-PVDF from the present study, grouped according to their symmetry. In reading the table, it is important to note that each molecular mode belonging to the A' or A'' species of the site symmetry C_s splits into two modes in the crystal, one being infrared active and the other Raman active (B_u split with A_g and A_u split with B_g). This is caused by the intermolecular interactions between the chains. For comparison, we have included the experimentally observed frequencies (measured at room temperature) along with those from

Table 3
Theoretical and experimental vibrational frequencies for α-poly(vinylidene fluoride)

Species	Present	Previous[a]		PED (%)[b]
		Observed	Calculated	
A_g	3068	2990	3042	$\nu_a(CH_2)$ (99)
	3010	2970	2975	$\nu_s(CH_2)$ (99)
	1402	1430	1455	$\delta(CH_2)$ (54) − $w(CH_2)$ (31)
	1354	1402	1392	$\delta(CH_2)$ (29) + $w(CH_2)$ (29) − $\nu_a(CC)$ (24)
	1294	1296	1279	$\nu_a(CF_2)$ (53) − $r(CF_2)$ (15)
	1149	1150	1158	$\nu_a(CC)$ (30) − $\nu_s(CF_2)$ (24)
	1078	1058	1083	$\nu_s(CF_2)$ (35) + $w(CH_2)$ (17)
	1014	976	973	$t(CH_2)$ (82)
	835	876	880	$\nu_s(CC)$ (38) + $\delta(CCC)$ (22)
	829	841	834	$r(CH_2)$ (48)
	584	612	617	$\delta(CF_2)$ (24) − $\delta'(CCC)$ (19)
	464	488	513	$\delta(CF_2)$ (48) + $w(CF_2)$ (25)
	392	414	434	$r(CF_2)$ (53) + $r(CH_2)$ (19)
	279	287	304	$t(CF_2)$ (54) + $w(CF_2)$ (18)
	200	206	231	$t(CF_2)$ (38) − $\delta(CCC)$ (19) + $\delta'(CCC)$ (18)
	65	75	77	τ_a (28) + τ_s (23) + $\delta(CCC)$ (20) + $r(CF_2)$ (18)
	51	52	59	$L(T_a)$
	48	29	11	$L(T_c)$
A_u	3071	3017	3040	$\nu_a(CH_2)$ (100)
	3016	2977	2977	$\nu_s(CH_2)$ (99)
	1407	NR	1477	$\delta(CH_2)$ (49) − $w(CH_2)$ (28)
	1337	1383	1359	$\delta(CH_2)$ (39) + $w(CH_2)$ (22)
	1254	1209	1241	$\nu_a(CF_2)$ (41) + $w(CH_2)$ (26)
	1151	1182	1199	$\nu_s(CF_2)$ (39) + $t(CH_2)$ (16)
	1117	1067	1069	$\nu_s(CC)$ (65)
	913	NR	934	$t(CH_2)$ (60) − $\nu_a(CF_2)$ (21)
	849	878	918	$\nu_a(CC)$ (60) + $\nu_s(CF_2)$ (20)
	768	795	818	$r(CH_2)$ (78)
	741	766	774	$\delta(CF_2)$ (33) − $\delta(CCC)$ (21)
	508	531	529	$\delta(CF_2)$ (52)
	389	389	407	$r(CF_2)$ (52)
	339	355	372	$t(CF_2)$ (63) + $r(CF_2)$ (16)
	275	215[c]	283	$\delta(CCC)$ (33) + $\delta'(CCC)$ (28) + $r(CF_2)$ (15)
	174	176	120	τ_a (71)
	55	53	51	$L(R_c^{\pi})$
B_g	3072	3030	3040	$\nu_a(CH_2)$ (100)
	3016	2980	2977	$\nu_s(CH_2)$ (99)
	1403	1442	1477	$\delta(CH_2)$ (49) − $w(CH_2)$ (28)
	1342	1384	1360	$\delta(CH_2)$ (39) + $w(CH_2)$ (22)
	1253	1200	1241	$\nu_a(CF_2)$ (41) + $w(CH_2)$ (26)
	1161	1190	1198	$\nu_s(CF_2)$ (39) + $t(CH_2)$ (16)
	1116	1064	1069	$\nu_s(CC)$ (65)
	913	940	935	$t(CH_2)$ (60) − $\nu_a(CF_2)$ (21)
	854	885	917	$\nu_a(CC)$ (60) + $\nu_s(CF_2)$ (20)
	769	800	815	$r(CH_2)$ (78)
	733	766	776	$\delta(CF_2)$ (33) − $\delta(CCC)$ (21)
	510	536	528	$\delta(CF_2)$ (52)
	389	NR	398	$r(CF_2)$ (52)
	339	357	371	$t(CF_2)$ (63) + $r(CF_2)$ (16)
	276	216[c]	283	$\delta(CCC)$ (33) + $\delta'(CCC)$ (28) + $r(CF_2)$ (15)
	174	176	130	τ_a (71)
	103	99	84	$L(T_b)$
	64	NR	62	$L(R_c^0)$
B_u	3068	3017	3042	$\nu_a(CH_2)$ (99)
	3011	2977	2975	$\nu_s(CH_2)$ (99)
	1401	1420	1456	$\delta(CH_2)$ (54) − $w(CH_2)$ (31)
	1353	1399	1392	$\delta(CH_2)$ (29) + $w(CH_2)$ (29) − $\nu_a(CC)$ (24)
	1291	1290	1278	$\nu_a(CF_2)$ (53) − $r(CF_2)$ (15)
	1130	1149	1159	$\nu_a(CC)$ (30) − $\nu_s(CF_2)$ (24)
	1077	1056	1083	$\nu_s(CF_2)$ (35) + $w(CH_2)$ (17)

Table 3
(*continued*)

Species	Present	Previous[a]		PED (%)[b]
		Observed	Calculated	
	1004	976	975	$t(CH_2)$ (82)
	832	873	877	$\nu_s(CC)$ (38) + $\delta(CCC)$ (22)
	831	853	835	$r(CH_2)$ (48)
	584	612	621	$\delta(CF_2)$ (24) − $\delta'(CCC)$ (19)
	465	489	509	$\delta(CF_2)$ (48) + $w(CF_2)$ (25)
	392	410	423	$r(CF_2)$ (53) + $r(CH_2)$ (19)
	279	288	309	$t(CF_2)$ (54) + $w(CF_2)$ (18)
	203	208	247	$t(CF_2)$ (38) − $\delta(CCC)$ (19) + $\delta'(CCC)$ (18)
	105	100	94	τ_a (28) + τ_s (23) + $\delta(CCC)$ (20) + $r(CF_2)$ (18)

Frequencies are given in cm^{-1}. NR indicates that an absorbance was not reported.
[a] From Ref. [23] at room temperature.
[b] Potential energy distribution from Ref. [23]. See Ref. [42] for notation. The sign (+/−) indicates the phase relation among the symmetry coordinates.
[c] See text for discussion of this mode.

semi-empirical force constant analysis [23]. Included in the semi-empirical calculations were modified intramolecular force constants (valence-field type) of Boerio and Koenig [19,20] and intermolecular force constants. The latter force constants were found from the combination of a Lennard–Jones potential (for the hydrogen–fluorine van der Waals interaction) and Coulombic force constants due to CF_2 dipole interactions between neighboring chains. The potential energy distribution for each vibrational frequency is also given (for mode notation see Ref. [42]). It should be noted that the reported experimental frequencies are based on spectra of real samples that possess some amount of head-to-head linkages or regions of non-crystallinity. These features affect the broadness of the spectral bands and also provide additional absorbencies [23]. Therefore a certain amount of variability is present in the experimental values.

We find very good agreement between our theoretical frequencies and those from experiment and semi-empirical calculations based on transferred force constants (see above). For most absorbencies, we find errors in the range of approximately ±5% compared to experiment. We found similar agreement to experiment using these same methods in our determination of the vibrational frequencies for the β-phase [40]. The A_u mode found experimentally at 215 cm^{-1} along with B_g mode at 216 cm^{-1} deserves particular attention. The presence of monomer inversion as the source of these modes has been mentioned in the literature [43]. Frequencies approximately 60 cm^{-1} higher than experiment were found in the present work and in the semi-empirical determination. A 272 cm^{-1} mode was also reported by Boerio and Koenig [20]. None of these models included monomer inversion.

Both the present work and the semi-empirical determination display a similar amount of error when compared with experiment for a majority of the vibrational spectrum. Exceptions to this occur at the low-frequency end. In this region, most of our frequencies are in much better agreement with experiment as compared to the semi-empirical results (e.g.: A_g: 279 cm^{-1}, 200 cm^{-1}, 51 cm^{-1}; A_u: 174 cm^{-1}; B_g: 174 cm^{-1}, 103 cm^{-1}; B_u: 279 cm^{-1}, 203 cm^{-1}, 105 cm^{-1}). It is this low-frequency or "soft" region of the vibrational spectrum that is considered to play a substantial role in ferroelectric phase transitions in perovskite-based materials [44–47]. The more accurate description of this portion of the vibrational spectrum in the present study will be crucial in modeling the dependency of molecular motions to strain in PVDF [48,49]. It has also been shown that the lower frequency modes provide a large contribution to dielectric response in perovskite ferroelectric materials [50].

When comparing our results to those of the semi-empirical/quantum-mechanical or CNDO methods [25], several factors must be considered. In the CNDO study, a single finite chain of α-PVDF was modeled. Therefore no intermolecular interactions were included in the calculation of the infrared vibrational spectrum. In addition, Correia and Ramos utilized the Hartree–Fock approximation. It is their contention that by parameterizing the CNDO calculations with experimental data, it is possible to incorporate to some extent the correlation energy of the system [51]. Since only graphical results were reported, quantitative comparison with our work is not possible. However, several comments can be made. In the CNDO study, a single absorbency was found at ~4500 cm^{-1} and large band of absorbencies was found between 2100 and 2400 cm^{-1}. There are no absorbencies reported in these regions experimentally, semi-empirically or in our work. The existence of these absorbencies results from documented over-prediction of force constants by a factor between 2 and 3 in CNDO calculations [52,53]. It is also possible that the lack of intermolecular interactions in the CNDO study resulted in the poor agreement. This so-called "collective polarization" enhancement in PVDF is only present when periodic crystals are studied which include intermolecular interactions [54]. Omission of this enhancement in β-PVDF semi-empirical models yielded values for the magnitude of the spontaneous polarization much lower than what is reported from periodic *ab initio* calculations [39,55]. Similarly, the modeling of an isolated chain of α-PVDF will not include the dipole of the neighboring chain in the unit cell that will be equal in magnitude but opposite in direction to yield the non-polar material. This may also explain why the semi-empirical vibrational frequencies, which only included two

intermolecular interactions, were not as accurate when compared to the present work at low frequencies where intermolecular interactions are more important.

4. Conclusions

The structure and vibrational frequencies of α-poly(vinylidene fluoride) have been determined using density-functional theory and periodic boundary conditions. Our relaxed structure shows very good agreement with experiment. The vibrational spectra found using density-functional perturbation are comparable in accuracy to the semi-empirical frequencies found from an experimentally parameterized potential fit. However, in the lower frequency spectral region, we find a higher level of agreement to experimental than the semi-empirical determination. Vibrational modes in this portion of the spectrum will be important for modeling phase transitions in α-PVDF and dielectric response. Comparison of our results to a previous semi-empirical/quantum-mechanical determination of the infrared spectrum shows the need to utilize a periodic array of PVDF chains in order to model the intermolecular interactions accurately and capture collective polarization effects.

Acknowledgements

The authors would like to thank Andrew M. Rappe and Joseph Bennett for helpful discussions. This work was supported by a grant from the Research Committee of the C.W. Post Campus of Long Island University. Funding for computational support was provided by Long Island University.

References

[1] Lovinger A. Science 1983;220:1115–21.
[2] Hasegawa R, Kobayashi M, Tadokoro H. Polym J 1972;3:591–9.
[3] Davis GT, McKinney JE, Broadhurst MG, Roth SC. J Appl Phys 1978; 49:4998–5002.
[4] Takahashi Y, Tadokoro H, Odajima A. Macromolecules 1980;13: 1320–2.
[5] Matsushige K, Nagata K, Imada S, Takemura T. Polymer 1980;21: 1391–7.
[6] Seisler HW. J Polym Sci B 1985;23:2413–22.
[7] Weinhold S, Bachmann MA, Litt MH, Lando JB. Macromolecules 1982; 15:1631–3.
[8] Doll WW, Lando JB. J Macromol Sci Phys B 1970;4:309–29.
[9] Hasegawa R, Takahashi Y, Chatani Y, Tadokoro H. Polym J 1972;3: 600–10.
[10] Bachmann MA, Lando JB. Macromolecules 1981;14:40–6.
[11] Takahashi Y, Kohyama M, Matsubara Y, Iwane H, Tadokoro H. Macromolecules 1981;14:1841–2.
[12] Farmer BL, Hopfinger AJ, Lando JB. J Appl Phys 1972;43:4293–303.
[13] Takahashi Y, Matsubara Y, Tadokoro H. Macromolecules 1983;16: 1588–92.
[14] Kutschabsy L, Höhne E, Kretschmer RG. Acta Polym 1991;42:357–9.
[15] Makarevich NI, Nikitin VN. Polym Sci (USSR) 1965;7:1843–9.
[16] Enomoto S, Kawai Y, Sugita M. J Polym Sci A 2 1968;6:861–9.
[17] Wentink T, Willworth LJ, Phaneuf JP. J Polym Sci 1961;55:551–62.
[18] Cortili G, Zerbi G. Spectrochim Acta 1967;23A:285–99.
[19] Boerio FJ, Koenig JL. J Polym Sci A 2 1969;7:1489–94.
[20] Boerio FJ, Koenig JL. J Polym Sci A 2 1971;9:1517–23.
[21] Synder RG. J Chem Phys 1967;47:1316–60.
[22] Boerio FJ, Koenig JL. J Chem Phys 1970;52:4826–9.
[23] Kobayashi M, Tashiro K, Tadokoro H. Macromolecules 1975;8:158–71.
[24] Nallasamy P, Mohan S. Indian J Pure Appl Phys 2005;43:821–7.
[25] Correia HMG, Ramos MMD. Comput Mater Sci 2005;33:224–9.
[26] The ABINIT programs are a common project of the Université Catholique de Louvain, Corning Inc. and other contributors (see http://www.abinit.org).
[27] For a description of the ABINIT project, Gonze X, Beuken JM, Caracas R, Detraux F, Fuchs M, Rignanese GM, et al. Comput Mater Sci 2002; 25:478–92; Gonze X, Rignanese GM, Verstraete M, Beuken JM, Pouillon Y, Caracas R, et al. Z Kristallogr 2005;220:558–62.
[28] Perdew JP, Burke K, Ernzerhof M. Phys Rev Lett 1996;77:3865–8.
[29] Rappe AM, Rabe KM, Kaxiras E, Joannopoulos JD. Phys Rev B 1990; 41:R1227–30.
[30] For OPIUM pseudopotential generation programs, see http://opium.sourceforge.net.
[31] Monkhorst HJ, Pack JD. Phys Rev B 1976;13:5188–92.
[32] Press WH, Flannery BP, Teukolsky SA, Vetterling WT. Numerical recipes in C. 2nd ed. Cambridge: Cambridge University Press; 1992.
[33] (a) Hellmann H. Einfuhrung in die quantumchemie. Leipzig: Deuticke; 1937;
(b) Feynman RP. Phys Rev 1939;56:340–3.
[34] Baroni S, Giannozzi P, Testa A. Phys Rev Lett 1987;58:1861–4.
[35] Gonze X, Allan DC, Teter MP. Phys Rev Lett 1992;68:3603–6.
[36] Gonze X. Phys Rev B 1997;55:10337–54.
[37] Gonze X, Lee C. Phys Rev B 1997;55:10355–68.
[38] Baroni S, de Gironcoli S, Dal Corso A, Giannozzi P. Rev Mod Phys 2001;73:515–62.
[39] Ramer NJ, Stiso KA. Polymer 2005;46:10431–6.
[40] Ramer NJ, Raynor CM, Stiso KA. Polymer 2006;47:424–8.
[41] Su H, Strachan A, Goddard III WA. Phys Rev B 2004;70:064101.
[42] Normal mode notation: ν_a (antisymmetric stretching); ν_s (symmetric stretching); δ (bending); w (wagging); r (rocking); t (twisting); δ (CCC) (skeletal bending of C1–C2–C1); δ' (CCC) (skeletal bending of C2–C1–C2); τ_a (antisymmetric combination of two torsional modes of C2–C1–C2–C1); τ_s (symmetric combination of two torsional modes of C2–C1–C2–C1); $L(T_i)$ (translational lattice mode for axis i); $L(R_c^0)$, $L(R_c^\pi)$ (librational lattice modes around the fiber axis c, with phase difference of 0 and π between the two chains in the unit cell, respectively). See text for atom identification.
[43] Rabolt JF, Johnson KW. J Chem Phys 1973;59:3710–2.
[44] Cochran W. Adv Phys 1960;9:387–423.
[45] DiDomenico M, Wemple SH, Porto SPS, Bauman RP. Phys Rev 1968; 174:522–30.
[46] Yamada Y, Shirane G, Linz A. Phys Rev 1969;2:848–57.
[47] Shirane G, Axe JD, Harada J, Remeika JP. Phys Rev B 1970;2:155–9.
[48] Sy JW, Mijovic J. Macromolecules 2000;33:933–46.
[49] Lanceros-Méndez S, Moreira MV, Mano JF, Schmidt VH, Bohannan G. Ferroelectrics 2002;273:15–20.
[50] Cockayne E. J Eur Ceram Soc 2003;23:2375–9.
[51] Ramos MMD, Correia HMG, Lanceros-Méndez S. Comput Mater Sci 2005;33:230–6.
[52] Sadley J. Semi-empirical methods in quantum chemistry. Chichester: Ellis Horwood; 1985.
[53] Pople JA, Beveridge DL. Approximate molecular orbital theory. New York: McGraw-Hill; 1970.
[54] Nakhmanson SM, Nardelli MB, Bernholc J. Phys Rev B 2005;72: 115210.
[55] Nakhmanson SM, Nardelli MB, Bernholc J. Phys Rev Lett 2004;92: 115504.